

Optimizing a-DCF for Spoofing-Robust Speaker Verification

Oğuzhan Kurnaz, Jagabandhu Mishra, Tomi H. Kinnunen, and Cemal Hanilçi

Abstract—Automatic speaker verification (ASV) systems are vulnerable to spoofing attacks such as text-to-speech. In this study, we propose a novel spoofing-robust ASV back-end classifier, optimized directly for the recently introduced, architecture-agnostic detection cost function (a-DCF). We combine a-DCF and binary cross-entropy (BCE) losses to optimize the network weights, combined by a novel, straightforward detection threshold optimization technique. Experiments on the ASVspoof2019 database demonstrate considerable improvement over the baseline optimized using BCE only (from minimum a-DCF of 0.1445 to 0.1254), representing 13% relative improvement. These initial promising results demonstrate that it is possible to adjust an ASV system to find appropriate balance across the contradicting aims of user convenience and security against adversaries.

Index Terms—a-DCF, spoofing-robust speaker verification

I. INTRODUCTION

Automatic speaker verification (ASV) seeks to verify a claimed identity based on speech evidence [1]. Despite being a matured biometric technology, ASV is susceptible to *spoofing* through replay [2], text-to-speech [3] and other adversaries. To counter these risks, various *countermeasures* (CMs) or *presentation attack detectors* (PADs) [4], have been proposed for detecting spoofing. Typically CMs are developed in isolation from ASV, and the two subsystems are combined to enhance robustness of the biometric system against adversaries. The common strategies include tandem (cascade) combination [5] and fusion of detection scores [6] or embeddings [7], [8]. Besides systems constructed from combination of speaker and spoof detection subsystems, other studies consider deep end-to-end networks optimized to predict the decision directly from the speech inputs [9], [10].

Whether realized by combining two subsystems (ASV and CM), or by training a monolithic end-to-end model, a key consideration is how to evaluate and optimize the complete biometric authentication system. Any such system must trade-off between misses (false rejections) and false alarms (false acceptances)—proxies for user (in)convenience and security, respectively. The so-called *tandem detection cost function* (t-DCF) [5] can be used to evaluate the performance of cascaded combinations of ASV and CM under a Bayes-risk framework.

O. Kurnaz, J. Mishra, and T. H. Kinnunen are with the School of Computing, University of Eastern Finland, Joensuu, Finland.

O. Kurnaz is also with the Department of Mechatronics Engineering, Bursa Technical University, Bursa, Turkey.

C. Hanilçi is with the Department of Electrical and Electronics Engineering, Bursa Technical University, Bursa, Turkey.

Corresponding author: Oğuzhan Kurnaz (oguzhan.kurnaz@btu.edu.tr).

This study has been partially supported by the Academy of Finland (Decision No. 349605, project "SPEECHFAKES"). The authors wish to acknowledge CSC – IT Center for Science, Finland, for computational resources.

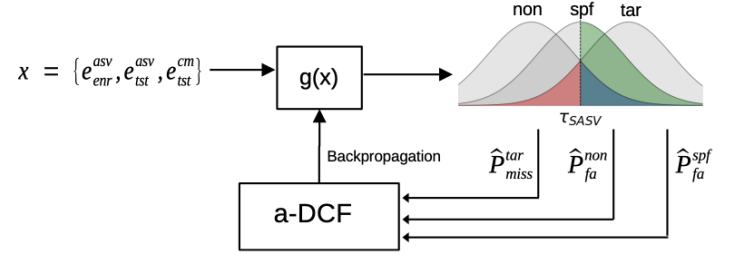


Fig. 1. Proposed a-DCF optimization method for spoofing-robust speaker verification. The model $g(x)$ takes embeddings as input and outputs score distributions, from which error rates \hat{P}_{miss}^{tar} , \hat{P}_{fa}^{non} , and \hat{P}_{fa}^{spf} are calculated. These error rates are then used to compute soft a-DCF, which serve as the loss function for model optimization through backpropagation, ensuring improved performance by minimizing the a-DCF.

Nonetheless, as t-DCF requires two sets of detection scores (and two detection thresholds) corresponding to the ASV and the CM subsystems, it is inapplicable for performance assessment of other types of architectures. To address these limitations, [11] proposed recently an *architecture-agnostic detection cost function* (a-DCF) applicable to a wider variety of system architectures. Unlike t-DCF, a-DCF requires a single detection score and a single threshold value only. This new metric is the primary metric in one of the two main tracks in the currently running ASVspoof 5 challenge¹.

For the first time, we propose a spoofing-robust ASV back-end that is directly optimized for the new a-DCF metric (as shown in Fig. 1). As an evaluation metric based on hard error counting, the original a-DCF metric is non-differentiable and cannot be directly optimized using gradient descent schemes. Luckily, hard error counts can be “softened” (made differentiable). While direct optimization of the t-DCF was addressed in [12] through reinforcement learning, this approach is limited to the tandem architectures. By integrating a differentiable version of the a-DCF into model training, we aim to enhance the performance and robustness of speaker verification systems against spoofing attacks, ultimately contributing to the advancement of secure and reliable biometric authentication technologies. Besides integrating the a-DCF metric into model training, the threshold value is also jointly optimized during model training in the proposed method.

II. DETECTION COST FUNCTIONS

Conventional *detection cost functions* [13] are evaluation metrics used to assess the performance of binary classification

¹<https://www.asvspoof.org/> (referred June 28, 2024)

systems, such as speaker verification and anti-spoofing. They focus on balancing the trade-off between *false alarms* and *misses*, assigning specific costs to each type of error. A binary classifier can be defined as a function $g : \mathcal{X} \rightarrow \mathbb{R}$ that assigns a detection score $g(x)$ for a given input $x \in \mathcal{X}$. This score then can be converted into predicted binary class label $\hat{y} \in \{0, 1\}$ by comparing it with a pre-set threshold τ by $\hat{y} = \mathbb{I}(g(x) > \tau)$. Here, \mathbb{I} is the indicator function which returns 1 if the condition is true (null hypothesis accepted) and 0 otherwise. In conventional ASV, x consists of a pair of enrollment and test utterances (presented typically as a pair of speaker embeddings), and the null hypothesis is that the same speaker is present in both. In our *spoofing-aware* ASV models, x additionally contains spoof embedding extracted from the test utterance by a CM model.

A. DCF and a-DCF

Detection Cost Function (DCF) [13] is used for performance assessment of conventional ASV systems. It is defined as:

$$\text{DCF}(\tau_{\text{asv}}) = C_{\text{miss}}^{\text{tar}} \cdot \pi_{\text{tar}} \cdot P_{\text{miss}}^{\text{tar}}(\tau_{\text{asv}}) + C_{\text{fa}}^{\text{non}} \cdot \pi_{\text{non}} \cdot P_{\text{fa}}^{\text{non}}(\tau_{\text{asv}}), \quad (1)$$

where $C_{\text{miss}}^{\text{tar}}$ is the cost of a miss, $C_{\text{fa}}^{\text{non}}$ is the cost of a false alarm, $P_{\text{miss}}^{\text{tar}}$ is the miss rate, $P_{\text{fa}}^{\text{non}}$ is false alarm rate, π_{tar} is the prior probability of the target and $\pi_{\text{non}} = 1 - \pi_{\text{tar}}$ is the prior probability of nontarget, and τ_{asv} is the detection threshold. The DCF in Eq. (1) allows one to set the cost parameters according to the user's application specification.

The architecture-agnostic detection cost function (a-DCF) [11] is a performance metric introduced for spoofing-aware speaker verification (SASV) task. It extends upon the DCF in Eq. (1) by including a third class (spoofing attack):

$$\begin{aligned} \text{a-DCF}(\tau_{\text{asv}}) = & C_{\text{miss}}^{\text{tar}} \cdot \pi_{\text{tar}} \cdot P_{\text{miss}}^{\text{tar}}(\tau_{\text{asv}}) \\ & + C_{\text{fa}}^{\text{non}} \cdot \pi_{\text{non}} \cdot P_{\text{fa}}^{\text{non}}(\tau_{\text{asv}}) \\ & + C_{\text{fa}}^{\text{spf}} \cdot \pi_{\text{spf}} \cdot P_{\text{fa}}^{\text{spf}}(\tau_{\text{asv}}), \end{aligned} \quad (2)$$

where $P_{\text{fa}}^{\text{spf}}$ is the false alarm for spoof trials, π_{spf} is the prior probability of spoofing, $C_{\text{fa}}^{\text{spf}}$ is the respective costs for spoof false alarms. τ_{asv} is the detection threshold for spoofing-aware speaker verification (SASV) system.

The miss rate ($P_{\text{miss}}^{\text{tar}}$) and the false alarm rates ($P_{\text{fa}}^{\text{non}}$, $P_{\text{fa}}^{\text{spf}}$) in the a-DCF metric are computed as follows:

$$\begin{aligned} P_{\text{miss}}^{\text{tar}}(\tau_{\text{asv}}) &= \frac{1}{N_{\text{tar}}} \sum_{x \in \text{tar}} \mathbb{I}(g(x) \leq \tau_{\text{asv}}) \\ P_{\text{fa}}^{\text{non}}(\tau_{\text{asv}}) &= \frac{1}{N_{\text{non}}} \sum_{x \in \text{non}} \mathbb{I}(g(x) > \tau_{\text{asv}}) \\ P_{\text{fa}}^{\text{spf}}(\tau_{\text{asv}}) &= \frac{1}{N_{\text{spf}}} \sum_{x \in \text{spf}} \mathbb{I}(g(x) > \tau_{\text{asv}}), \end{aligned} \quad (3)$$

where N_{tar} , N_{non} , and N_{spf} represent the number of target, non-target, and spoof class trials, respectively.

B. Differentiable a-DCF Metric

The indicator function used to compute false alarm and miss rates in Eq. (3) is non-differentiable. Therefore, the a-DCF metric can not be directly used as loss function to optimize an

SASV system. In this study, we propose a differentiable (soft) version of a-DCF suitable for direct minimization using gradient descent. Similar approaches have been successfully applied to optimize DCF for text-dependent speaker verification [14] and t-DCF for the constrained class of tandem systems [15], but not the a-DCF. The a-DCF metric provides a more holistic evaluation by integrating the costs associated with speaker verification. This approach simplifies the benchmarking process for different ASV system architectures, as it eliminates the need for separate metrics for each component. By focusing on a single metric, the a-DCF metric promotes development of integrated systems that are optimized for spoofing-aware speaker verification.

The non-differentiable components in a-DCF metric are the miss rate ($P_{\text{miss}}^{\text{tar}}$) and the two false alarm rates ($P_{\text{fa}}^{\text{non}}$, $P_{\text{fa}}^{\text{spf}}$). A common approach for 'softening' hard error counts [14], [15] is to replace the indicator function by a continuous, differentiable function. We adopt the following approximations:

$$\begin{aligned} \hat{P}_{\text{miss}}^{\text{tar}}(\tau_{\text{asv}}) &= \frac{1}{N_{\text{tar}}} \sum_{x \in \text{tar}} \sigma(\tau_{\text{asv}} - g(x)) \\ \hat{P}_{\text{fa}}^{\text{non}}(\tau_{\text{asv}}) &= \frac{1}{N_{\text{non}}} \sum_{x \in \text{non}} \sigma(g(x) - \tau_{\text{asv}}) \\ \hat{P}_{\text{fa}}^{\text{spf}}(\tau_{\text{asv}}) &= \frac{1}{N_{\text{spf}}} \sum_{x \in \text{spf}} \sigma(g(x) - \tau_{\text{asv}}), \end{aligned} \quad (4)$$

where $\sigma(z) = \frac{1}{1+e^{-z}}$ is the sigmoid function. Essentially, the error rates are approximated based on their distance from the threshold. The soft a-DCF loss is now defined as:

$$\begin{aligned} \mathcal{L}_{\text{a-DCF}}^{\text{soft}}(\tau_{\text{asv}}) = & C_{\text{miss}}^{\text{tar}} \cdot \pi_{\text{tar}} \cdot \hat{P}_{\text{miss}}^{\text{tar}}(\tau_{\text{asv}}) \\ & + C_{\text{fa}}^{\text{non}} \cdot \pi_{\text{non}} \cdot \hat{P}_{\text{fa}}^{\text{non}}(\tau_{\text{asv}}) \\ & + C_{\text{fa}}^{\text{spf}} \cdot \pi_{\text{spf}} \cdot \hat{P}_{\text{fa}}^{\text{spf}}(\tau_{\text{asv}}). \end{aligned} \quad (5)$$

C. Optimization of soft a-DCF

Algorithm 1 Optimization Algorithm

```

1: Input: Train data  $\mathcal{D}_{\text{trn}}$ , Development data  $\mathcal{D}_{\text{dev}}$ , Batch Size  $B$ ,
   Number of Epochs  $N$ 
2: Output: Best threshold  $\hat{\tau}_*$ , Model Parameters  $\Theta_*$ 
3: Initialize:  $\text{min\_a-DCF} \leftarrow \infty$ ,  $\tau \leftarrow 0.5$ 
4: for epoch = 1 to  $N$  do
5:   // optimize DNN weights
6:   for  $X \leftarrow \text{get\_minibatch}(\mathcal{D}_{\text{trn}}, B)$  do
7:      $\mathcal{J}(\Theta_i, \tau_i) \leftarrow (\mathcal{L}_{\text{a-DCF}}^{\text{soft}}(X; \Theta_i, \tau_i) + \mathcal{L}_{\text{BCE}}(X; \Theta_i)) / 2$ 
8:      $\Theta_{i+1} \leftarrow \text{update\_network\_weights}(\Theta_i, \mathcal{J}(\Theta_i, \tau_i))$ 
9:   end for
10:   $\Theta \leftarrow \Theta_{i+1}$ 
11:  // find optimal threshold using grid search
12:   $\tau_{i+1} \leftarrow \underset{\tau}{\text{argmin}} \{ \mathcal{L}_{\text{a-DCF}}^{\text{soft}}(\Theta, \tau) \}$  in  $\mathcal{D}_{\text{trn}}$ 
13:  // keep track of best model using dev data
14:  if  $\mathcal{L}_{\text{a-DCF}}^{\text{soft}}(\tau_{i+1}) < \text{min\_a-DCF}$  in  $\mathcal{D}_{\text{dev}}$  then
15:     $\text{min\_a-DCF} \leftarrow \mathcal{L}_{\text{a-DCF}}^{\text{soft}}(\tau_{i+1})$ 
16:     $\hat{\tau} \leftarrow \tau_{i+1}$ 
17:  end if
18: end for
19: return  $\hat{\tau}_*$ ,  $\Theta_*$ 

```

The algorithm 1 presents the training loop of a neural network towards its optimization, with both soft a-DCF

($\mathcal{L}_{\text{a-DCF}}^{\text{soft}}(X; \Theta_i, \tau_i)$) and BCE loss ($\mathcal{L}_{\text{BCE}}(X; \Theta_i)$) functions. The BCE loss is the binary cross entropy loss defined as:

$$\mathcal{L}_{\text{BCE}} = -\frac{1}{N} \sum_{i=1}^N [y_i \log(\hat{y}_i) + (1 - y_i) \log(1 - \hat{y}_i)] \quad (6)$$

where N represents the number of training samples. Essentially, the soft a-DCF loss is a loss function of application dependent a-DCF metric and useful for fine-tuning the system towards a desired miss-false alarm balance. The BCE loss, in turn, helps to separate target from the pool of the two negative classes. For these reasons, we use the combination of these two losses. The algorithm initializes a minimum a-DCF to be infinity and a fixed threshold τ . Then, for each epoch, it optimizes the model weights by calculating the combined loss $\mathcal{J}(\Theta_i, \tau_i)$ from soft a-DCF and BCE losses and updating the weights of the neural network. This combined loss is defined as:

$$\mathcal{J}(\Theta_i, \tau_i) = \frac{1}{2} \left(\mathcal{L}_{\text{a-DCF}}^{\text{soft}}(\tau_{\text{sasv}}) + \mathcal{L}_{\text{BCE}} \right). \quad (7)$$

The algorithm then conducts a grid search (Line 12 in Algorithm 1) for a value of τ that gives the optimal threshold according to the a-DCF loss on the training data. The threshold value serves as the independent variable in Eq. (5) of the a-DCF loss. Using the a-DCF loss (or its combination with BCE loss) as the objective function during model training involves minimizing its value, which depends on the threshold value. This relationship necessitates finding the optimal threshold value that minimizes the a-DCF loss at each epoch which is achieved through grid search. This algorithm tracks the best model parameters and threshold as scored on development data, thus updating the lowest a-DCF found so far and its corresponding parameters. At the end, it returns the best threshold $\hat{\tau}_*$ and model parameters Θ_* .

III. EXPERIMENTAL SETUP, RESULTS AND DISCUSSION

We perform experiments on the ASVspoof2019 logical access (LA) [3] dataset. The description of the dataset and experimental details are discussed in the following subsections.

A. Dataset

The ASVspoof2019 LA subset consists of three parts, training, development, and evaluation. Each partition has a disjoint set of speakers. The average duration of the utterances is 2 to 3 seconds. The spoofed utterances are generated using 19 VC and TTS algorithms (6 types of attacks in the training and the development sets, 13 in the evaluation set).

B. Experimental Setup

To demonstrate our proposed optimization scheme, we consider the DNN-based embedding fusion strategy 'Baseline2' described in [7], that was used as a baseline in the SASV2022 challenge. Thereafter, many other studies follow similar approach to perform SASV [16], [17]. We aim to show whether our proposed technique brings any performance improvement or not. This model concatenates three embeddings ($\mathbf{e} = [\mathbf{e}_{\text{enr}}^{\text{asv}}, \mathbf{e}_{\text{tst}}^{\text{asv}}, \mathbf{e}_{\text{tst}}^{\text{cm}}]$): two speaker (ASV) embeddings

from the enrolment ($\mathbf{e}_{\text{enr}}^{\text{asv}}$) and test ($\mathbf{e}_{\text{tst}}^{\text{asv}}$) utterances extracted using ECAPA-TDNN [18], and one spoofing (CM) embedding ($\mathbf{e}_{\text{tst}}^{\text{cm}}$) extracted from the test utterance using AASIST [19]. The concatenated embeddings are fed to a DNN model that consists of three fully connected hidden layers with leaky ReLU activation functions. The layers contain 256, 128, and 64 neurons, respectively. Unlike baseline, which contains two neurons with softmax, our model's final layer contains a single neuron with a sigmoid activation function. This is because of our a-DCF optimization requires only one output score.

We consider four back-end models that are otherwise identical but optimized differently. These methods are:

- **S1**: corresponds to the Baseline2 system provided by SASV challenge organizers (optimized with CE);
- **S2**: optimized using soft a-DCF loss with, $\tau_{\text{sasv}} = 0.5$;
- **S3**: optimized using soft a-DCF loss + BCE, with $\tau_{\text{sasv}} = 0.5$;
- **S4**: optimized using soft a-DCF loss + BCE, including threshold optimization, as detailed in Algorithm 1.

The cost values $C_{\text{miss}}^{\text{tar}}$, $C_{\text{fa}}^{\text{non}}$, and $C_{\text{fa}}^{\text{spf}}$ in the soft a-DCF calculation are set as 1, 10, and 20, respectively, while the prior values π_{tar} , π_{non} , and π_{spf} are set as 0.9, 0.05, and 0.05. The higher relative cost value for spoof false alarms ($C_{\text{fa}}^{\text{spf}} = 20$) is chosen based on the importance of spoofing robustness in security-sensitive domains, such as banking, where preventing unauthorized access is crucial. This reflects the emphasis to penalize false acceptance of spoof attempts to ensure the integrity and security of such systems. Additionally, the high target prior ($\pi_{\text{tar}} = 0.9$) indicates that the system is designed under the assumption that most interactions are legitimate. This is practical for applications where legitimate access attempts are frequent, and it minimizes the disruption to bonafide users by reducing the likelihood of false rejections. Except training, we considered the a-DCF metric given in Eq. 2 in all the experiments for performance evaluation.

TABLE I
BASELINE SYSTEM MIN *a*-DCF VALUES IN THE DEVELOPMENT SET

Batch size	24	48	96	192	384	768	1024
min a-DCF	0.1437	0.1308	0.1268	0.1346	0.1297	0.1251	0.1234

C. Baseline (S1)

We firstly trained a baseline (**S1**) with cross entropy loss for various batch sizes, resulting to minimum a-DCF values shown in Table I. The results indicate that the best performance was achieved with a batch size of 1024. We fix this value for the remainder of the experiments.

TABLE II
COMPARISON OF S1 AND S2 IN DEVELOPMENT SET. BATCH SIZE IS SELECTED AS 1024.

System	min a-DCF
S2	0.1355
S3	0.1182

D. Proposed *a*-DCF metric optimization (S2, S3 and S4)

We next consider models **S2** and **S3**, beginning with the hard-coded detection threshold of $\tau_{\text{sasv}} = 0.5$ in Eq. (5).

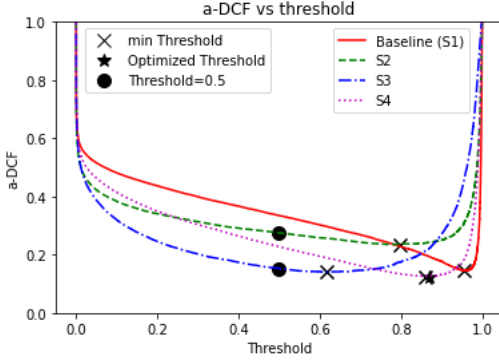


Fig. 2. The plot illustrates the a-DCF values with respect to the threshold for the four different systems. The curves represent the a-DCF values for *Baseline* (S1), S2, S3, and S4 systems across various threshold values. Circular markers indicate the a-DCF values at a fixed threshold of 0.5 for each system. Cross markers denote the minimum a-DCF values and their corresponding threshold points. The star marker represents the optimized threshold and the corresponding a-DCF value proposed for the S4 system.

Model selection is based on the lowest a-DCF value at a threshold of 0.5 in the development set. The soft a-DCF only system (S2) attains minimum a-DCF of 0.1355 and the combination of the soft a-DCF and BCE (S3) achieves minimum a-DCF of 0.1182 as summarized in Table II.

TABLE III

COMPARISON OF S1, S2, S3, AND S4 IN DEVELOPMENT AND EVALUATION SET. THE RESULTS ARE GIVEN USING 1024 AS BATCH SIZE.

	Baseline (S1)	S2	S3	S4
Dev	0.1234	0.1355	0.1182	0.1109
Eval	0.1445	0.2352	0.1398	0.1254

The results of S2 and S3 were based on hard-coded arbitrary detection threshold of $\tau_{\text{sasv}} = 0.5$. We now also optimize τ_{sasv} using the complete procedure (Algorithm 1). Joint optimization of the DNN parameters and the threshold leads to noticeable improvements, as expected. Specifically, S4 achieved a minimum a-DCF of 0.1109 on the development set and 0.1254 on the evaluation set, outperforming S1, S2, and S3 as Table III indicates.

Fig. 2 illustrates the a-DCF curves obtained for the four different systems (S1, S2, S3, and S4) as a function of the threshold. For systems S2 and S3, the a-DCF values at both the fixed threshold value of 0.5 and their respective minimum points are depicted on the graph. For the S4 system, that includes threshold optimization, the a-DCF value corresponding to the optimized threshold is marked with a star. As can be seen from the graph (and supported by the results), the S4 model provides the lowest a-DCF value.

E. Impact of a-DCF Parameter

Our final analysis addresses the impact of the a-DCF parameters. To this end, we introduced three different set of a-DCF parameters as:

- **Setting1 (soft a-DCF)** contains only a-DCF loss. In this case, the cost values $C_{\text{miss}}^{\text{tar}}$, $C_{\text{fa}}^{\text{non}}$, and $C_{\text{fa}}^{\text{spf}}$ are set to 1, 10, and 20, respectively. The prior values π_{tar} , π_{non} , and π_{spf} are set to 0.9, 0.05, and 0.05.

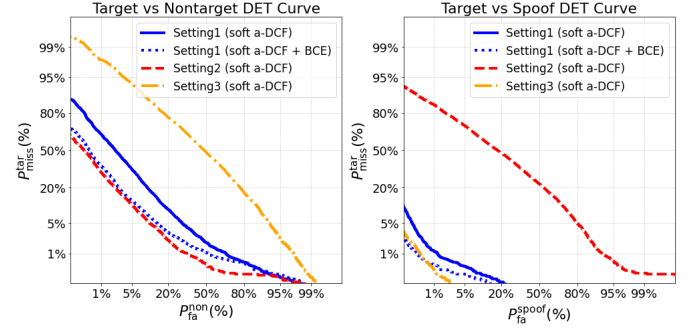


Fig. 3. Target vs Nontarget and Target vs Spoof DET curves for three different a-DCF parameter settings. The SV-EER values for *Setting1* (represented by the solid blue line), *Setting1* (soft a-DCF + BCE) (represented by the dotted blue line), *Setting2*, and *Setting3* are **13.97%**, **8.44%**, **7.52%**, and **49.13%**, respectively.

- **Setting1 (soft a-DCF + BCE)** contains both a-DCF and BCE losses. The cost and the prior values are the same as in the previous case.
- **Setting2 (soft a-DCF)** contains only a-DCF loss. In this case, the cost values $C_{\text{miss}}^{\text{tar}}$, $C_{\text{fa}}^{\text{non}}$, and $C_{\text{fa}}^{\text{spf}}$ are all set to 1. The prior values π_{tar} , π_{non} , and π_{spf} are set to 0.5, 0.5, and 0, respectively.
- **Setting3 (soft a-DCF)** contains only a-DCF loss. The same cost values are used as in the previous setting, while 0.5, 0 and 0.5 priors are used for π_{tar} , π_{non} , and π_{spf} , respectively.

The threshold optimization method was included for all these cases. Fig. 3 shows target vs. nontarget and target vs. spoof DET profiles for three different sets of a-DCF parameters. The figure clearly indicates that the choice of a-DCF parameters significantly impacts both DET profiles. Comparing *setting1*'s soft a-DCF alone with the soft a-DCF combined with BCE, the former generally has a lower miss rate. For *setting2* and *setting3*, changes in the priors cause notable differences in the DET curves. For example, setting π_{spf} to 0 (*setting2*), assuming no spoof non-targets, shows the best performance for target vs. nontarget trials across all operating points. However, when the non-target prior is set to 0 (*setting3*), the performance for target vs. nontarget trials is found to be inferior, as expected. These trends are reversed for target vs. spoof trials.

IV. CONCLUSION

In this study, we demonstrated that a spoofing-aware speaker verification system can be effectively optimized for the new a-DCF metric. By incorporating both the a-DCF and binary cross-entropy losses in the optimization process, we fine-tuned the network weights, which led to improved performance over the baseline system. Importantly, the usage of a novel threshold optimization technique further enhanced the system's capabilities, resulting in a significant improvement in a-DCF values. These findings highlight the potential for adjusting ASV systems to achieve an optimal balance between user convenience and security against to evolving spoofing attacks.

REFERENCES

- [1] D. A. Reynolds, "Speaker identification and verification using Gaussian mixture speaker models," in *Proc. ESCA Workshop on Automatic Speaker Recognition, Identification and Verification*, 1994, pp. 27–30.
- [2] T. Kinnunen, M. Sahidullah, H. Delgado, M. Todisco, N. Evans, J. Yamagishi, and K. Lee, "The asvspoof 2017 challenge: Assessing the limits of replay spoofing attack detection," in *Proc. Interspeech 2017*, 2017, pp. 2–6.
- [3] M. Todisco, X. Wang, V. Vestman, M. Sahidullah, H. Delgado, A. Nautsch, J. Yamagishi, N. Evans, T. Kinnunen, and K. A. Lee, "Asvspoof 2019: Future horizons in spoofed and fake audio detection," 2019.
- [4] ISO/IEC 30107-1:2023, "Information technology biometric presentation attack detection." [Online]. Available: <https://www.iso.org/standard/83828.html>
- [5] T. Kinnunen, H. Delgado, N. Evans, K. A. Lee, V. Vestman, A. Nautsch, M. Todisco, X. Wang, M. Sahidullah, J. Yamagishi *et al.*, "Tandem assessment of spoofing countermeasures and automatic speaker verification: Fundamentals," *IEEE/ACM Transactions on Audio, Speech, and Language Processing*, vol. 28, pp. 2195–2210, 2020.
- [6] M. Todisco, H. Delgado, K. A. Lee, M. Sahidullah, N. Evans, T. Kinnunen, and J. Yamagishi, "Integrated Presentation Attack Detection and Automatic Speaker Verification: Common Features and Gaussian Backend Fusion," in *Proc. Interspeech 2018*, 2018, pp. 77–81.
- [7] H. jin Shim, H. Tak, X. Liu, H.-S. Heo, J. weon Jung, J. S. Chung, S.-W. Chung, H.-J. Yu, B.-J. Lee, M. Todisco, H. Delgado, K. A. Lee, M. Sahidullah, T. Kinnunen, and N. Evans, "Baseline systems for the first spoofing-aware speaker verification challenge: Score and embedding fusion," 2022. [Online]. Available: <http://arxiv.org/abs/2204.09976>
- [8] X. Liu, M. Sahidullah, K. A. Lee, and T. Kinnunen, "Generalizing speaker verification for spoof awareness in the embedding space," 1 2024. [Online]. Available: <http://arxiv.org/abs/2401.11156>
- [9] W. Kang, M. J. Alam, and A. Fathan, "End-to-end framework for spoof-aware speaker verification," in *Proc. Interspeech 2022*, 2022, pp. 4362–4366.
- [10] Z. Teng, Q. Fu, J. White, M. E. Powell, and D. C. Schmidt, "Sa-sasv: An end-to-end spoof-aggregated spoofing-aware speaker verification system," pp. 2–6, 2022. [Online]. Available: <http://arxiv.org/abs/2203.06517>
- [11] H. jin Shim, J. weon Jung, T. Kinnunen, N. Evans, J.-F. Bonastre, and I. Lapidot, "a-DCF: an architecture agnostic metric with application to spoofing-robust speaker verification," *arXiv preprint, submitted to Odyssey: the Speaker and Language Recognition Workshop*, 2024.
- [12] A. Kanervisto, V. Hautamäki, T. Kinnunen, and J. Yamagishi, "Optimizing tandem speaker verification and anti-spoofing systems," 1 2022. [Online]. Available: <http://arxiv.org/abs/2201.09709><http://dx.doi.org/10.1109/TASLP.2021.3138681>
- [13] G. R. Doddington, M. A. Przybicki, A. F. Martin, and D. A. Reynolds, "The NIST speaker recognition evaluation – overview, methodology, systems, results, perspective," *Speech Communication*, vol. 31, no. 2, pp. 225–254, 2000.
- [14] V. Mingote, A. Miguel, D. Ribas, A. Ortega, and E. Lleida, "Optimization of False Acceptance/Rejection Rates and Decision Threshold for End-to-End Text-Dependent Speaker Verification Systems," in *Proc. Interspeech 2019*, 2019, pp. 2903–2907.
- [15] A. Kanervisto, V. Hautamäki, T. Kinnunen, and J. Yamagishi, "Optimizing tandem speaker verification and anti-spoofing systems," *IEEE/ACM Transactions on Audio, Speech, and Language Processing*, vol. 30, pp. 477–488, 2021.
- [16] Y. Zhang, G. Zhu, and Z. Duan, "A probabilistic fusion framework for spoofing aware speaker verification," 2022. [Online]. Available: <http://arxiv.org/abs/2202.05253>
- [17] L. Zhang, Y. Li, H. Zhao, Q. Wang, and L. Xie, "Backend ensemble for speaker verification and spoofing countermeasure," *arXiv preprint arXiv:2207.01802*, 2022.
- [18] B. Desplanques, J. Thienpondt, and K. Demuynck, "Ecapa-tdnn: Emphasized channel attention, propagation and aggregation in tdnn based speaker verification," in *Proc. Interspeech 2020*. ISCA, Oct. 2020. [Online]. Available: <http://dx.doi.org/10.21437/Interspeech.2020-2650>
- [19] J.-w. Jung, H.-S. Heo, H. Tak, H.-j. Shim, J. S. Chung, B.-J. Lee, H.-J. Yu, and N. Evans, "Aasist: Audio anti-spoofing using integrated spectro-temporal graph attention networks," in *Proc. ICASSP 2022-2022 IEEE International Conference on Acoustics, Speech and Signal Processing (ICASSP)*. IEEE, 2022, pp. 6367–6371.